A 6-GHz 80-W GaAs FET Amplifier with a TM-Mode Cavity Power Combiner

YASUYUKI TOKUMITSU, MEMBER, IEEE, TOSHIYUKI SAITO, MEMBER, IEEE, NAOFUMI OKUBO, AND YOSHIAKI KANEKO

Abstract—A novel 8-way divider/combiner using TM_{010}- and TM_{020}-mode cavities was developed. This divider/combiner has an insertion loss of 0.2 dB and a bandwidth of 600 MHz in the 6-GHz communications band.

For broadening the operating bandwidth of the divider/combiner, two techniques of double cavities and tight coupling are described. Degradation of power-combining efficiency is also discussed when input signals into a power combiner have variations in amplitude and phase.

By using this divider/combiner, an experimental 6-GHz 80-W GaAs FET amplifier with a combining efficiency of 85 percent was demonstrated to investigate the feasibility of a solid-state high-power amplifier.

I. Introduction

HIGH-POWER GaAs FET amplifiers delivering an output power of about 10 W have recently been used in many types of practical microwave communications equipment. GaAs FET amplifiers have the advantages of having a lower voltage power supply, higher reliability, and a reduced size and weight when compared with traveling-wave tube (TWT) amplifiers [1], [2].

At the microwave frequencies, however, since we can only obtain devices with an output power of several watts, it is difficult to manufacture a solid-state high-power amplifier delivering an output power over 50 W. Therefore, the output power of many devices must be combined to make a high-power amplifier. In other words, a power combiner is the key component in a solid-state high-power amplifier.

Many kinds of power combiners have been reported [1], [3]–[6]. The most conventional power combiner is the corporate structure combiner which uses a number of 3-dB hybrids. This structure has the disadvantages of a higher insertion loss and a large size. Although a multi-way power combiner constructed with microwave integrated circuit technology reduces the size, it does not have the capability for the operating power level. A resonant-cavity-type power combiner is the best of all combiners, we believe, because it overcomes these problems. The resonant-cavity-type combiner previously reported has, however, a narrow bandwidth as its weak point.

This paper begins by describing techniques for broadening the operating bandwidth of an N-way power divider/combiner composed of TM-mode double cavities. Based on these techniques, the newly developed 8-way divider/combiner has an insertion loss of 0.2 dB and a bandwidth of 600 MHz at 6 GHz.

A discussion of the effects on combining efficiency in phase and amplitude variations of input signals to the combiner is also included.

The design and performance of unit amplifiers are also presented.

Finally, a 6-GHz 80-W GaAs FET amplifier with a combining efficiency of 85 percent is demonstrated to investigate the feasibility of a solid-state high-power amplifier.

Manuscript received June 8, 1983; revised December 13, 1983.
The authors are with Fujitsu Laboratories Ltd., Kawasaki, 211 Japan.

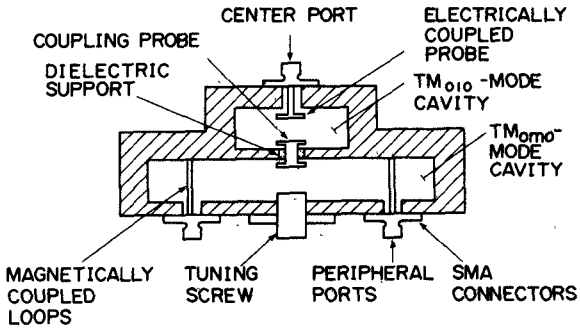

Fig. 1. Schematic diagram of N-way divider/combiner.

II. TM-Mode Cavity Power Divider/Combiner

The TM_{0m0}-mode is suitable for use as the resonant-cavity-type divider/combiner as it is easy to separate the associated mode from other undesired resonant modes. It is also not difficult to obtain multi-ports because it has a constant electromagnetic field in the azimuthal direction.

A. Broadening Technique

1) Double Cavities: Fig. 1 is a schematic diagram of a newly proposed N-way divider/combiner using the TM-mode cavity. A double tuned circuit composed of TM_{010}- and Tm_{0m0}-mode cavities is used to get a broad bandwidth. The center port is electrically coupled with a disk-type probe to the TM_{010}-mode cavity for tight coupling, and peripheral ports are magnetically coupled with loops to the TM_{0m0}-mode cavity for getting multi-ports of N. Two cavities are mutually coupled with a disk-type probe.

0018-9480/84/0300-0301$01.00 ©1984 IEEE

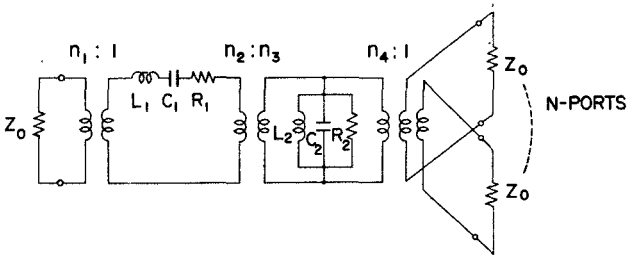

Fig. 2. Equivalent circuit of the N-way divider/combiner.

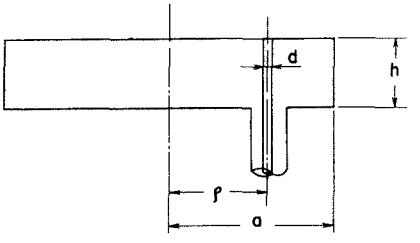

Fig. 3. Cross section of a cavity having a single peripheral port for analyzing the coupling coefficient of the loop.

The equivalent circuit of this divider/combiner can be represented as in Fig. 2. Although the disk-type probe can be coupled easily to the cavity, the loop cannot be tightly coupled. So, a bandwidth or loaded Q (Q_L) of the divider/combiner depends on coupling coefficients of peripheral loops.

When the coupling coefficient of the loop at the peripheral port is constant, a flat bandwidth or a 0.2-dB bandwidth for the double cavities can be expected to be about twice as wide as that of a single cavity, while a 3-dB bandwidth decreases by $1/\sqrt{2}$.

2) Tight Coupling: The other technique is tight coupling of the loop.

Let us now consider the coupling coefficient of a higher TM_{0m0}-mode cavity with a single loop as shown in Fig. 3. Analysis of a single cavity combiner has been reported in many papers [4], [7]. However, broadening the bandwidth has not been investigated. The analysis procedure used here and the calculated results will be described.

The electromagnetic field in the cylindrical coordinates is given by

$$\left.\begin{aligned} E_Z &= E_0 J_0(kr) \\ H_\phi &= j\frac{E_0}{\eta} J_1(kr) \\ k &= \frac{\chi_{0m}}{a} = \omega\sqrt{\epsilon_0\mu_0} \end{aligned}\right\} \tag{1}$$

where E_z is the electric field along the axis of the cavity, H_ϕ is the magnetic field in the azimuthal direction, k is a wave-number, E_0 is the amplitude of electric field at the center in the cavity, η is the intrinsic impedance, J_0 and J_1 indicate the zero- and first-order Bessel functions, χ_{0m} is mth root of $J_0(\chi) = 0$, r is the distance from the center axis, a is the radius of the cavity, ω is the angular frequency, ϵ_0 is the dielectric constant of free space, and finally, μ_0 is the permeability of free space.

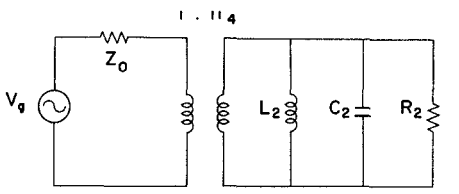

Fig. 4. Simplified equivalent circuit of the single-port cavity.

The stored energy in the cavity is expressed by

$$\begin{aligned} W_t &= \int_V \frac{\epsilon_0|E_z|^2}{4}dv + \int_V \frac{\mu_0|H_\phi|^2}{4}dv \\ &= \pi\epsilon_0 h\frac{a^2}{2}E_0^2 J_1^2(ka) \end{aligned} \tag{2}$$

where h is the height of the cavity.

The dissipation power due to imperfect conductivity is represented by

$$\begin{aligned} P_R &= 2\pi ah\frac{R_s}{2}|J_z|^2 + 2\int_0^a \frac{R_s}{2}|J_r|2\pi r\,dr \\ &= \frac{\pi aR_s E_0^2}{\eta^2}J_1^2(ka)\{h+a\} \end{aligned} \tag{3}$$

where R_s is surface resistivity of the cavity wall, J_z and J_r are the current densities in the direction of the z-axis and radius.

Consequently, the unloaded Q is given by

$$\begin{aligned} Q_0 &= \frac{\omega W_t}{P_R} \\ &= \frac{\eta ak}{2R_s\left(\frac{a}{h}+1\right)}. \end{aligned} \tag{4}$$

Combining (2), (3), and (4), the input admittance at the resonant frequency becomes the real part and is obtained in

$$\begin{aligned} G &= \left.\frac{2P_R}{|E_z|^2h^2}\right|_{r=\rho} \\ &= \frac{\pi a^2\omega\epsilon_0}{hQ_0}\left\{\frac{J_1(ka)}{J_0(k\rho)}\right\}^2 \end{aligned} \tag{5}$$

where ρ is the distance of the loop from the center axis.

The equivalent circuit of the cavity is expressed in a strict sense as the summation of many resonant circuits. But, in the vicinity of the frequency which excites the associated TM_{0m0}-mode, the equivalent circuit is simplified as in Fig. 4. The input admittance of the cavity loading a generator and the external Q are given by

$$Y_{\text{in}} = \frac{n_4^2C_2\left\{\omega_0^2 - \omega^2 + j\frac{\omega_0\omega}{Q_0}\right\}}{j\omega} \tag{6}$$

$$Q_E = \frac{Q_0}{\beta} \tag{7}$$

where

$$\left.\begin{aligned} Q_0 &= \omega_0 C_2 R_2 \\ \omega_0^2 &= \frac{1}{L_2 C_2} \\ \beta &= \frac{R_2}{n_4^2 Z_0}. \end{aligned}\right\} \tag{8}$$

Q_0 indicates the unloaded Q, ω_0 is the resonant angular frequency, and β shows the coupling coefficient. In the equations, n_4 is the transformation ratio of loop coupling, Z_0 is impedance of the generator, and L_2, C_2, and R_2 are inductance, capacitance, and resistance of the cavity.

At resonant frequency, the input admittance becomes only the real part of

$$G_{in} = \frac{n_4^2}{R_2}. \tag{9}$$

From (5), (8), and (9), the coupling coefficient of the peripheral port is determined in

$$\beta = \frac{2Q_0 h \eta \lambda_0}{Z_0} \left\{ \frac{J_0(k\rho)}{2\pi a J_1(ka)} \right\}^2 \tag{10}$$

where λ_0 is the wavelength at the resonant frequency.

In practice, the self-inductance of the coupling loop is not negligible. The effective coupling coefficient is expressed by

$$\beta' = \frac{\beta}{1 + \left(\frac{\omega L_e}{Z_0} \right)^2} \tag{11}$$

where L_e is the effective self-inductance of a shorted eccentric coaxial line with a length of h as follows:

$$L_e = \frac{Z_{0e}}{\omega} \tan(kh) \tag{12}$$

$$Z_{0e} = 60 \cosh^{-1} \left\{ \frac{1}{2} \left(\frac{4a^2 + d^2 - 4\rho^2}{2ad} \right) \right\} \tag{13}$$

where Z_{0e} indicates the characteristic impedance of the eccentric coaxial line.

The calculated results of external Q for TM_{020}-, TM_{030}-, and TM_{040}-modes are shown in Fig. 5. In calculation, surface resistivity is used in $2.52 \times 10^{-7} \sqrt{f}\,\Omega$ for silver. To get tight coupling of the loop or a broad bandwidth, it is clearly concluded as follows from these figures.

a) External Q shows the local minimum values against the distance of the coupling loop from the center of the cavity as shown in Fig. 5(a). Since these distances correspond to the local maximum points of the electric field, the coupling loop should be placed at the outermost local maximum point to prepare a large number of coupling ports.

b) Fig. 5(b) indicates that the height of the cavity should be low. In other words, a flat cavity must be adopted for broadening the bandwidth.

c) The diameter of the coupling loop should be wide as shown in Fig. 5(c).

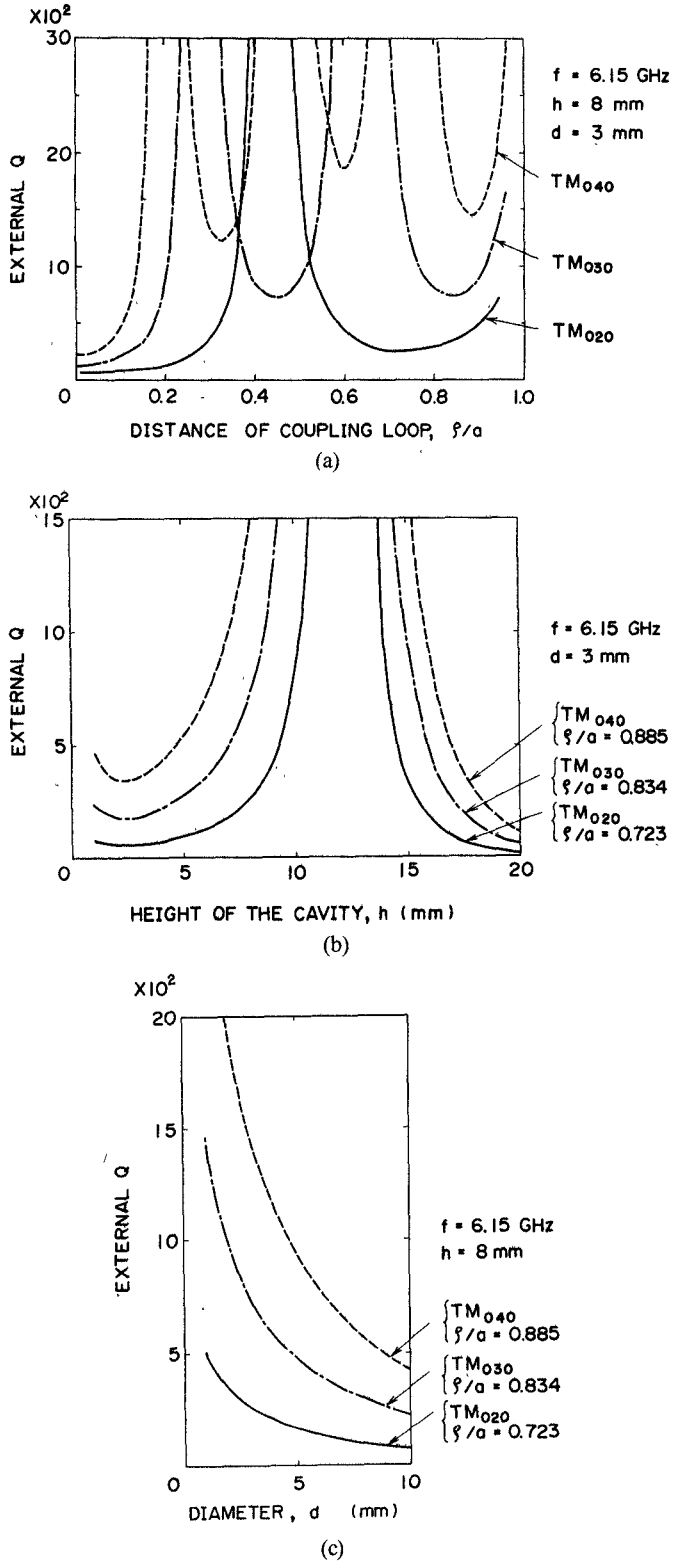

Fig. 5. Calculated external Q of the single-port cavity for the higher resonant modes of TM_{020}-, TM_{030}-, and TM_{040}-modes as a function of (a) the distance of the coupling loop from the center, (b) the height of the cavity, and (c) the diameter of the loop.

B. Design

For an efficient divider/combiner, we must consider not only the bandwidth, but also the insertion loss.

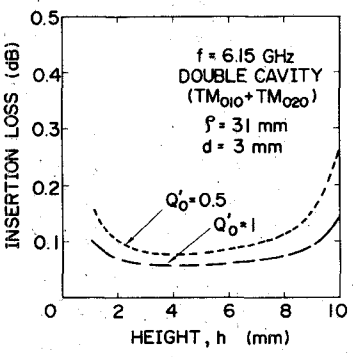

Fig. 6. Calculated insertion loss of 8-way double cavities ($TM_{010}+TM_{020}$) divider/combiner.

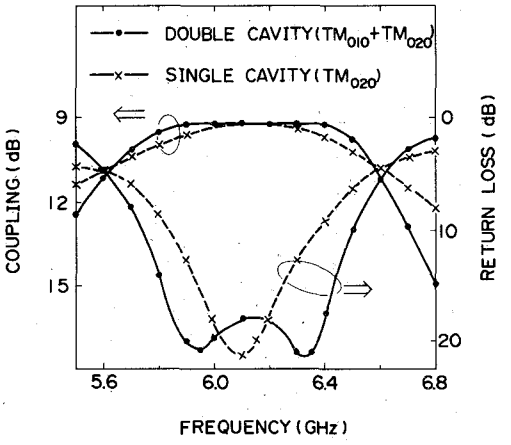

Fig. 7. Coupling and return loss of 8-way divider/combiner with double cavities ($TM_{010}+TM_{020}$) compared with that of a single cavity (TM_{020}). Coupling between a center port and one of the peripheral ports, along with return loss at a center port, are shown.

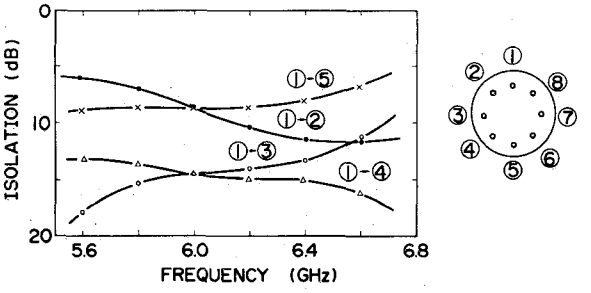

Fig. 8. Isolation between peripheral ports of 8-way divider/combiner.

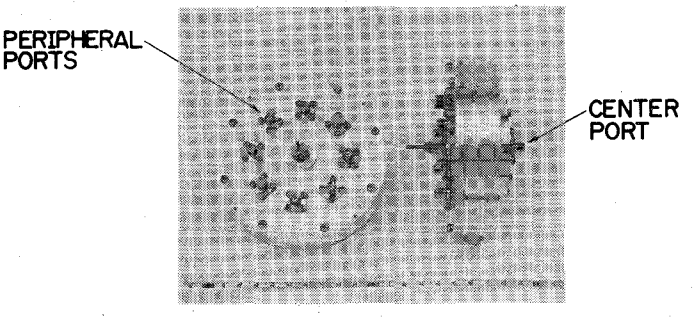

Fig. 9. External views of a developed 8-way divider/combiner.

The loaded Q of an N-way divider/combiner with double cavities is given by

$$Q_L = \frac{Q_E}{\sqrt{2}N} \tag{14}$$

where Q_E is an external Q with a single port, assuming a frequency response with Butterworth characteristics.

The calculated insertion loss characteristics of an 8-way divider/combiner using TM_{010}- and TM_{020}-mode cavities as a function of the height of the cavities are shown in Fig. 6. Q_0's are the unloaded Q normalized by the theoretical value. The insertion loss has a minimum value, and its characteristics are almost flat. The insertion loss increases due to the degradation of the unloaded Q at a low height and the increase of external Q at the greater height, respectively. The insertion loss of the divider/combiner does not greatly increase even if the unloaded Q of the cavity becomes half of the theoretical value.

From the theoretical results mentioned above, the design parameters on the construction of the TM_{020}-mode cavity would be determined. They are a cavity diameter of 83 mm, a cavity height of about 3 mm, a distance of the loop from the center axis of the cavity of 30 mm, and a loop diameter of more than 10 mm. However, the lower height of the cavity and the large diameter of the loop are difficult to fabricate, and the large diameter of the loop does not mechanically match the SMA connector. Considering the facts and the facility of fabrication, we finally designed an 8-way divider/combiner for a 6-GHz 80-W GaAs FET amplifier with the following dimensions:

TM_{010}-mode cavity (center port cavity): $2a = 36$ mm, $h = 8$ mm.

TM_{020}-mode cavity (peripheral port cavity): $2a = 83$ mm, $h = 8$ mm, $\rho = 31$ mm, $d = 3$ mm.

The coupling of the probe at the center port and mutual coupling between the two cavities in a double tuned circuit were determined experimentally.

C. Experimental Result

Fig. 7 shows the characteristics of an 8-way divider/combiner with double cavities ($TM_{010}+TM_{020}$). For reference, the characteristics of a divider/combiner with a single cavity (TM_{020}) are also shown. The divider/combiner with double cavities has a coupling of 9.2 dB between a center port and one of the peripheral ports. This results in a 0.2-dB insertion loss. A 0.2-dB bandwidth of 600 MHz has been achieved at 6 GHz, which is sufficient for the communications band. As the diagram shows, the bandwidth is twice as broad as the bandwidth of a single cavity. The return loss at the center port is more than 18 dB. The variation of the coupling is less than ± 0.1 dB and the transmission phase variation is less than ± 2 degrees. The isolation characteristics between peripheral ports are shown in Fig. 8. An isolation of more than 8.5 dB has been obtained. This value is smaller than the theoretical value of 18 dB, and is the reason why undesired modes are excited in the cavity. The return loss at peripheral ports was derived from the measured S-parameters because it is difficult to measure the return loss directly when in-phase

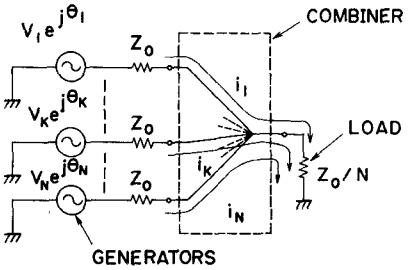

Fig. 10. Simplified equivalent circuit of the N-way lossless combiner.

and equal level excitation are the conditions at all peripheral ports. The return loss is more than 13 dB at 6.15 GHz.

Fig. 9 is a photograph of the experimental 8-way divider/combiner.

III. Discussion of Power-Combining Efficiency

In practice, unit amplifiers cannot avoid having variations in their output power and transmission phase even if the amplifiers have the same design and are produced in the same lot. So it is important to investigate the power-combining efficiency.

Assuming that the circuit has no loss, an equivalent circuit of the N-way combiner can be simplified as in Fig. 10.

The relationship between voltage and current in a kth circuit is given by

$$V_k e^{j\theta_k} = Z_0 i_k + \frac{Z_0}{N}(i_1 + \cdots + i_N) \tag{15}$$

where V_k is the amplitude of voltage for a kth generator, θ_k is the phase of voltage, i_k is the current, Z_0 is impedance of the generator, and Z_0/N is the load impedance.

From (15), the power dissipated in the load is obtained in

$$P_0 = |i_1 + \cdots + i_N|^2 \frac{Z_0}{N} = \frac{1}{4NZ_0}\left|\sum_{k=1}^{N} V_k e^{j\theta_k}\right|^2 \tag{16}$$

while the total generating power is given by

$$P_T = \frac{1}{4Z_0}\sum_{k=1}^{N} |V_k e^{j\theta_k}|^2. \tag{17}$$

Consequently, the power-combining efficiency is expressed by

$$\eta_c = \frac{P_0}{P_T} \times 100(\%) = \frac{\left|\sum_{k=1}^{N} V_k e^{j\theta_k}\right|^2}{N\sum_{k=1}^{N} V_k^2} \times 100(\%). \tag{18}$$

The calculated results of power-combining efficiency of the 8-way divider/combiner are shown in Fig. 11 as functions of the input power and phase variations. It is assumed that variations in the power and phase of the generator are distributed uniformly.

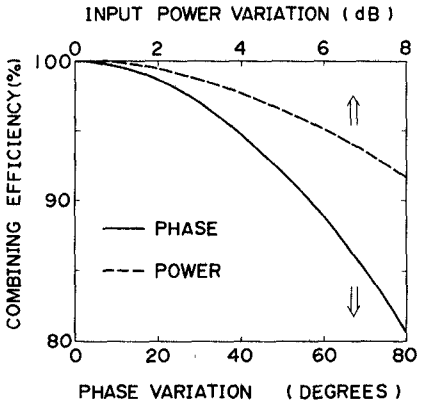

Fig. 11. Calculated power-combining efficiency for 8-way divider/combiner as a function of variations in power and phase of exciting generators.

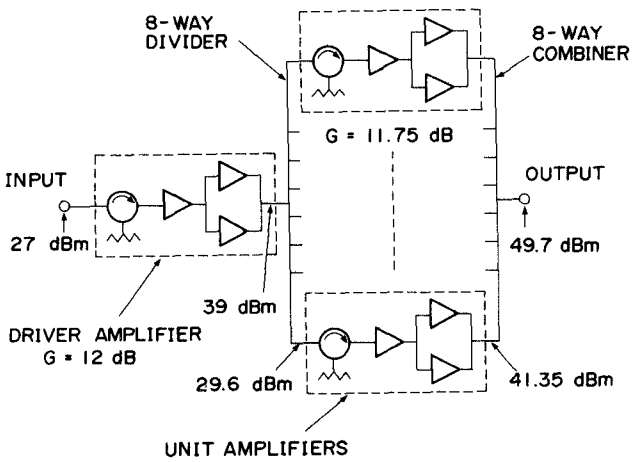

Fig. 12. Block diagram of an experimental 6-GHz 80-W GaAs FET amplifier.

From this figure, it is clearly concluded that the phase variation is more sensitive than the input power. To obtain a combining efficiency greater than 99 percent, the phase and power variation must be adjusted within 15 degrees and within 2.6 dB, respectively. In an experimental 6-GHz 80-W high-power amplifier represented in the next section, the variation in the transmission phase and the power of unit amplifiers has been adjusted within 6 degrees and within 0.5 dB.

IV. Experimental 6-GHz 80-W GaAs FET Amplifier

To investigate the feasibility of the developed 8-way power divider/combiner, a 6-GHz 80-W broad-band GaAs FET amplifier was used [8]. The amplifier combined the output power of eight unit amplifiers, and has a combining efficiency of 85 percent.

A. Configuration

Fig. 12 is a block diagram of the 80-W amplifier. This amplifier consists of a drive amplifier, eight unit amplifiers, a power divider, and a power combiner.

The unit amplifiers are kept separate for cooling, and are connected to the divider and the combiner with semi-rigid

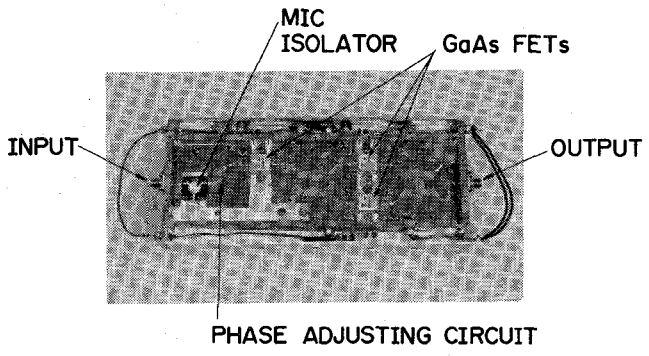

Fig. 13. Internal view of a unit amplifier with output power of more than 12 W and linear gain of more than 14 dB at 6.15 GHz.

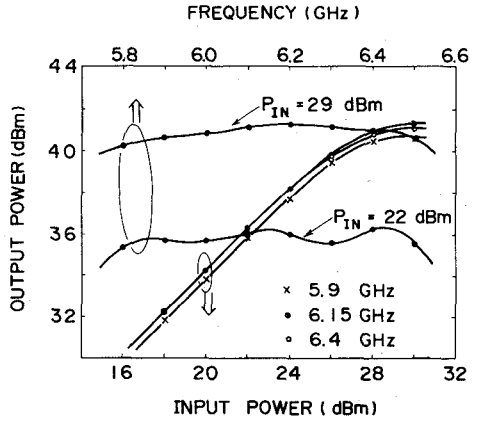

Fig. 14. Typical characteristics of a unit amplifier.

coaxial cables which have an insertion loss of 0.2 dB.

An amplifier that uses a divider/combiner such as this 80-W amplifier should be constructed so as to get high power efficiency and to reduce the number of transistors in order to keep the cost low and the reliability high.

The gain will need more than 10 dB if degradation of efficiency due to the insertion loss of the divider is taken into account. An excess gain results in a need for many transistors.

In this experimental amplifier, each unit is a two-stage amplifier with a 13-dB gain at the 1-dB gain compression point. A balanced amplifier in the final stage and an isolator in the input side are used to reduce the interference between unit amplifieres due to weak interport isolation in the divider/combiner.

The driver amplifier has the same configuration as the unit amplifier.

TABLE I
SUMMARIZED PERFORMANCE OF EIGHT UNIT AMPLIFIERS AT 6.15 GHz (INCLUDING DIVIDER)

AMPLIFIER NUMBER	f = 6.15 GHz, P_{IN} = 39 dBm	
	OUTPUT POWER (dBm)	PHASE (DEGREE)
1	41.3	-50
2	41.1	-51
3	41.4	-48
4	41.6	-51
5	41.5	-45
6	41.2	-49
7	41.2	-51
8	41.5	-50
AVERAGE	41.35 dBm	-48
VARIATION	0.5 dB	6
TOTAL	50.38 dBm	------

B. Unit Amplifier

An internal view of the unit amplifier is shown in Fig. 13. Internally matched GaAs FET's of FLM5964-5 and FLM5964-6 are used in the first and final stages, respectively. The device used in the final stage has an output power of 6 W and a gain of more than 5.5 dB at 6.4 GHz. The gate width is 22.8 mm and the I_{dss} is 4.4 A.

The balanced amplifier in the final stage uses two-section branch-line hybrids to obtain a broad bandwidth. An MIC isolator which has a 0.4-dB insertion loss is set in the input side.

To adjust the transmission phase of the unit amplifier, a phase adjusting circuit is prepared as shown in Fig. 13. This circuit has two 100-Ω lines of different lengths connected in parallel and has an adjusting range of around 90 degrees. The matching circuits and dc bias circuits are formed on a 0.8 mm-thick Teflon® glass-fiber substrate.

The typical frequency response of output power, and the output power as a function of the input power characteristics of the unit amplifier are shown in Fig. 14.

The frequency response of the amplifier is nearly flat in the frequency range between 5.9 GHz and 6.4 GHz. The amplifier has a linear gain of 14 dB and a saturated output power of more than 12 W.

Table I shows the characteristics of the eight unit amplifiers connected with an 8-way power divider which is excited by an input power of 39 dBm from the center port at 6.15 GHz.

The average output power is 41.35 dBm or 13.6 W and the total power is 50.38 dBm or 109.1 W. The output power variation between unit amplifiers is within 0.5 dB, and the transmission phase variation is adjusted to be within 6 degrees at 6.15 GHz when the phase adjusting circuit is used. These variations affect the combining efficiency by a factor of less than 0.2 percent. The return loss at the output port of unit amplifiers is more than 10 dB because of imbalances in the S-parameters between two internally matched devices. If the combining is done ideally, the output power of the 80-W amplifier is expected to be 50.37 dBm or 108.9 W.

C. Overall Performance

Fig. 15 shows the overall performance of the experimental 6-GHz 80-W GaAs FET amplifier with forced air cooling. The figure shows the frequency responses at linear and saturated points, and the output versus input power characteristics at three frequency points. A saturated output power of more than 49 dBm or 80 W is obtained over a frequency range of 5.9 GHz to 6.4 GHz. The linear gain is more than 26 dB. At a center frequency of 6.15 GHz, the saturated output power is 49.7 dBm or 93 W with a power

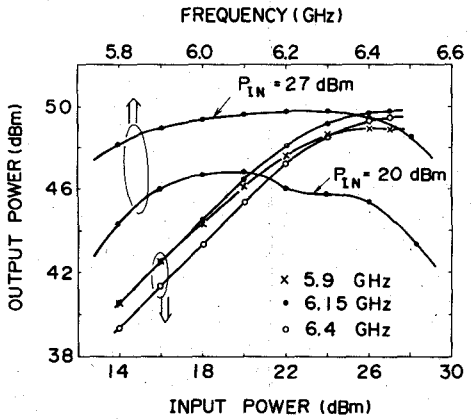

Fig. 15. Overall performance of the experimental 6-GHz 80-W GaAs FET amplifier using forced air cooling.

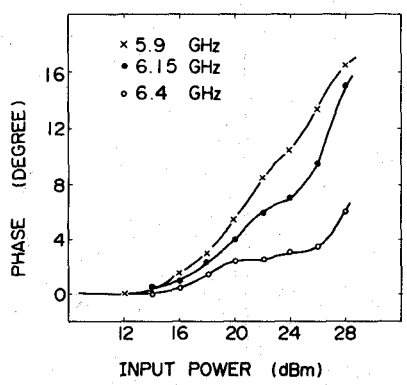

Fig. 16. Characteristics of AM-to-PM conversion for the experimental amplifier.

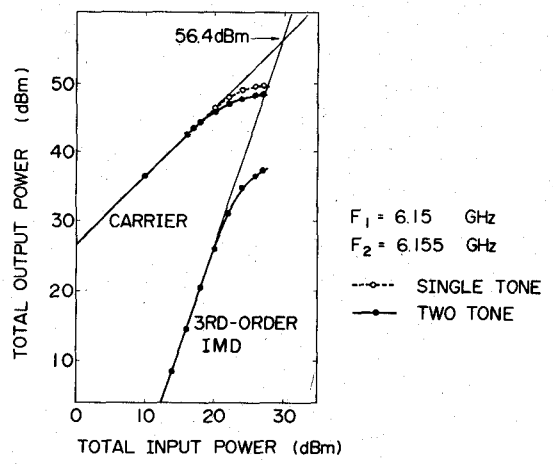

Fig. 17. Characteristics of third-order intermodulation distortion for the experimental amplifier.

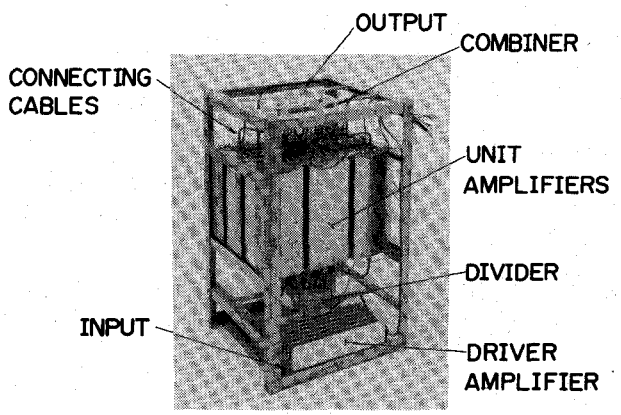

Fig. 18. External view of the experimental 6-GHz 80-W GaAs FET amplifier.

gain of 22.7 dB and a power efficiency of 18.9 percent. The overall power-combining efficiency is 85 percent. The loss factors are: insertion loss of the combiner, 0.2 dB; loss in the connecting cable from the unit amplifier to the combiner, 0.2 dB. The remaining loss factors of 0.3 dB are considered to arise from the mismatch loss between the unit amplifiers and combiner because the output impedance of the unit amplifiers is only 10 dB, and the input impedance (peripheral port) of the combiner is only 13 dB, as mentioned in Section II-C. When the impedance mismatch loss is reduced, this combining technique will provide a 0.4-dB loss or a 91-percent power-combining efficiency.

The characteristics of AM-to-PM conversion at three frequency points and the third-order intermodulation distortion at 6.15 GHz are shown in Figs. 16 and 17, respectively. A third-order intercept point of 56.4 dBm and an AM-to-PM conversion coefficient of less than 2.6 degree/dB are obtained. In the AM-to-PM conversion coefficient, this amplifier is superior to an equivalent TWT amplifier.

As mentioned above, because the total efficiency of this amplifier is about 18 percent, more than 400 W are being dissipated in this amplifier. In order to adequately cool the device, the amplifier uses forced air cooling equipment. The cooling equipment has four 12-cm fans with an air velocity of more than 6 km/h, and each unit amplifier has a radiator that is 800 cm^2. The temperature rise of the unit amplifier case is suppressed to within 20°C from the ambient temperature.

A photograph of the experimental 80-W amplifier without a cooling fan is shown in Fig. 18. This amplifier is 270 mm long, 250 mm wide, and 450 mm high.

The weight of this amplifier is 19 kg without the cooling equipment.

V. Conclusion

A novel 8-way divider/combiner using TM_{010}- and TM_{020}-mode cavities was developed. This divider/combiner has a low insertion loss of 0.2 dB and a broad bandwidth of 600 MHz in the 6-GHz communications band. This high performance was achieved by using two techniques of double cavities and tight coupling. These techniques can also be applied to a divider/combiner for high-power solid-state amplifiers in a frequency range higher than the *X*-band.

A 6-GHz 80-W GaAs FET amplifier was successfully demonstrated using the divider/combiner and eight unit amplifiers. The amplifier has a saturated output power of more than 80 W over the satellite communications band from 5.9 GHz to 6.4 GHz, and a high combining efficiency

of 85 percent. At a center frequency of 6.15 GHz, the saturated output power is 93 W.

Even in a high-power range over 100 W, the results suggest that, with improvements in the power-combining technique, a GaAs FET amplifier will surpass a TWT amplifier in the near future.

ACKNOWLEDGMENT

The authors are grateful to Dr. H. Komizo for supporting and encouraging this work.

REFERENCES

[1] K. Chang and C. Sun, "Millimeter-wave power-combining techniques," *IEEE Trans. Microwave Theory Tech.*, vol. MTT-31, pp. 91–107, Feb. 1983.
[2] D. Aubert, S. Dhillon, N. LaPadre, S. Moochalla, and J. Patel, "Power amps replace TWTAs in satellite transponders," *Microwave Syst. News*, vol. 13, pp. 62–76, Apr. 1983.
[3] K. J. Russell, "Microwave power combining techniques," *IEEE Trans. Microwave Theory Tech.*, vol. MTT-27, pp. 472–478, May 1979.
[4] M. Dydyk, "Efficient power combining," *IEEE Trans. Microwave Theory Tech.*, vol. MTT-28, pp. 755–762, July 1980.
[5] B. J. Sanders, "Radial combiner runs circles around hybrids," *Microwaves*, pp. 55–58, Nov. 1980.
[6] M. Cohn, B. D. Geller, and J. M. Schellenberg, "A 10 watt broadband FET combiner/amplifier," in *1979 IEEE MTT-S Int. Microwave Symp. Dig.*, pp. 292–297.
[7] R. Aston, "Techniques for increasing the bandwidth of a TM_{010}-mode power combiner," *IEEE Trans. Microwave Theory Tech.*, vol. MTT-27, pp. 479–482, May 1979.
[8] N. Okubo, Y. Kaneko, T. Saito, and Y. Tokumitsu, "A 6-GHz 80-W GaAs FET amplifier with TM-mode cavity power combiner," in *1983 IEEE MTT-S Int. Microwave Symp. Dig.*, pp. 276–278.

Yasuyuki Tokumitsu (M'78) was born in Shimonoseki, Japan, on May 16, 1943. He received the B.E. and M.E. degrees from Kyushu Institute of Technology, Kitakyushu, Japan, in 1966 and 1968, respectively.

In 1968, he joined Fujitsu Laboratories Ltd., Kawasaki, Japan, where he has been engaged in the research and development of passive and active components, and subsystems for microwave communications equipment. Currently, he is interested in millimeter-wave hybrid integrated circuits, millimeter-wave radio communications equipment, and low-noise and high-power solid-state amplifiers for satellite communications equipment. He is now leading the Radio and Satellite Communications System-Components Development Group in the Radio and Satellite Communications Systems Laboratory of Fujitsu Laboratories Ltd..

Mr. Tokumitsu is a member of the Institute of Electronics and Communication Engineers of Japan.

Toshiyuki Saito (M'82) was born in Mie, Japan, on August 11, 1945. He received the B.E. degree from Tokyo Denki University, Tokyo, in 1970, and the M.E. degree from Chiba University, Chiba, Japan, in 1972.

In 1972, he joined Fujitsu Laboratories Ltd., Kawasaki, Japan, where he was engaged in the research and development of microwave solid-state components for radio communication systems. Currently, he has been engaged in the research of low-noise and high-power solid-state amplifiers for satellite communications systems. He is now a Senior Engineer of the Radio and Satellite Communications Systems Laboratory, Integrated Communications Division, Fujitsu Laboratories Ltd..

Mr. Saito is a member of the Institute of Electronics and Communication Engineers of Japan.

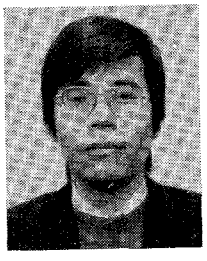

Naofumi Okubo was born in Asahigawa, Japan, on April 7, 1952. He received the B.E. and M.E. degrees in electronics engineering from Niigata University, Niigata, Japan, in 1976 and 1978, respectively.

In 1978, he joined Fujitsu Laboratories Ltd., Kawasaki, Japan, where he has been engaged in the research and development of high-power amplifiers for microwave communications equipment. He is now a Senior Engineer of the Radio and Satellite Communications Systems Laboratory, Integrated Communications Division, Fujitsu Laboratories Ltd..

Mr. Okubo is a member of the Institute of Electronics and Communication Engineers of Japan.

Yoshiaki Kaneko was born in Saitama, Japan, on July 15, 1957. He received the B.E. and M.E. degrees in electronics devices engineering from the Technological University of Nagaoka, Nagaoka, Japan, in 1980 and 1982, respectively.

In 1982, he joined Fujitsu Laboratories Ltd., Kawasaki, Japan, where he is engaged in research on microwave circuits and components.

Mr. Kaneko is a member of the Institute of Electronics and Communication Engineers of Japan.